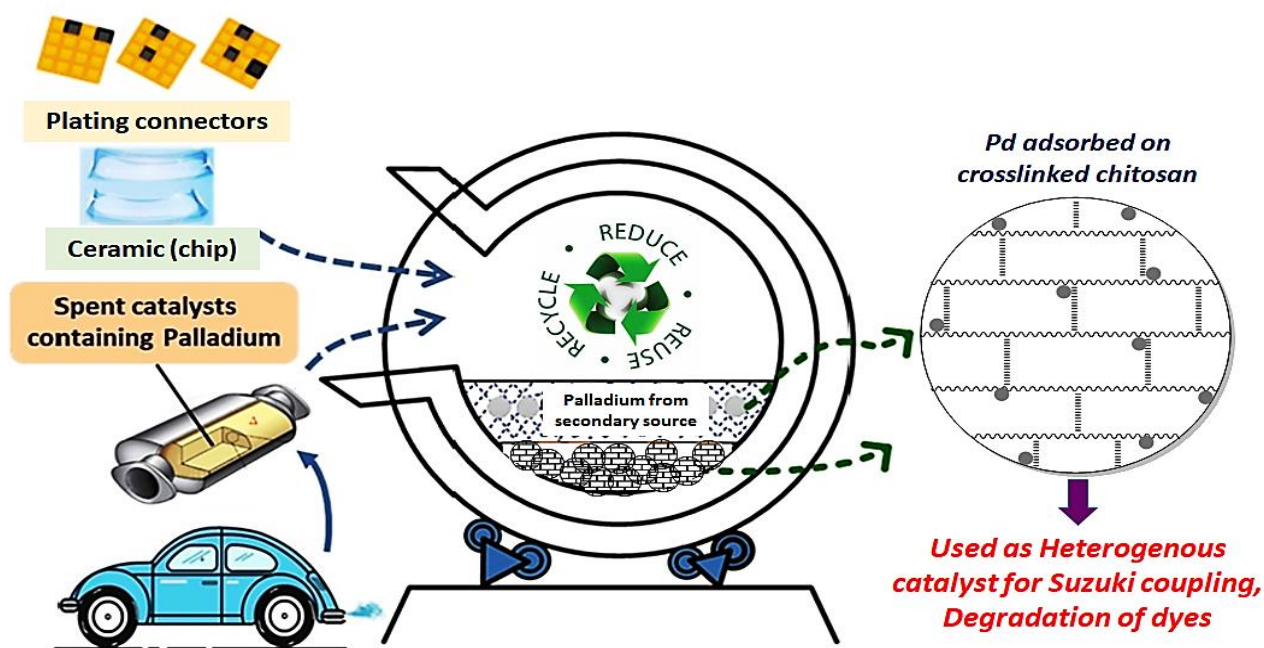




Chapter 4: Recovery of Pd from Electroless Plating Solution using Cross- Linked Chitosan Derivatives and its valorization as efficient heterogeneous Catalysts for Organic Synthesis and Environmental Remediation



4.1. Introduction

Palladium is a precious transition metal with wide applications in autocatalysis, medical devices and jewellery. Palladium is an important catalyst in wide range of organic transformations such as oxidation, reduction, Heck reaction, Suzuki coupling, Stille coupling, Sonogashira coupling, C-F bond formation, degradation of dyes and Nitrophenols etc. that find widespread implications in pharmaceutical and other chemical industries (Anjum et al., 2020; Leonhardt et al., 2010; Sahin & Gubbuk, 2022; Sargin et al., 2020)

Increased applicability of palladium has led to depletion of palladium sources and increased cost. The ever-rising demand supply gap for Pd due to reduction in resource availability in earth's crust is indicative of the requirements of Pd (II) recovery from spent resources and waste streams. From the environmental perspective, Pd accumulation in the environment is injurious to human health and can result in a number of illnesses, including eye irritation, asthma, rhino conjunctivitis and skin issues. Also, palladium has the capacity to be transported through plant roots and later could enter into the food chain (Nagarjuna et al., 2017). From both environmental and economical perspectives, it is thus imperative to effectively recover and utilize the available palladium in a sustainable manner and reuse it efficiently (Lee et al., 2021).

Pd can be recovered and reused from secondary sources such as catalytic converter, multi-layer ceramic (chip) capacitors, plating connectors and lead frames (Godlewska-Zytkiewicz et al., 2019). Electroless plating is an easy, low cost and inexpensive technique for depositing palladium. It produces uniformly required coatings from aqueous solutions on both conducting and non-conducting surfaces without applying the electrical external current and/or potential. (Cheng & Yeung, 2001). Electroless plating has been employed for Pd membrane production (Buekenhoudt et al., 2010). After membrane synthesis the spent solutions contains significant amount of Pd metal which needs to be recovered and reused. Electroless plating can thus become an attractive secondary source for Pd.

Numerous techniques like ion exchange, electrolysis, chemical precipitation, adsorption, leaching, and electrochemical reduction, membrane separation, biosorption, electro-kinetic process, magnetic nanoparticle-based process, foam fractionation, hydrothermal sulfidation, flotation, and molecular recognition gel technology have been used for recovery of palladium (Nagireddi et al., 2018). Amongst all the techniques, adsorption is an attractive alternative due to promising features such as faster kinetics, higher recovery at lower concentrations, ease of operation and low cost (Nagireddi et al., 2017). Japanese cedar wood powder was chemically

modified to a tertiary-amine-type adsorbent and studied for the selective recovery of Pd(II) from simulated high-level liquid waste indicating the suitability of the adsorbent for various industrial waters (Parajuli & Hirota, 2009).

Ca-alginate immobilized *p.vermicola* has been applied as a biosorbent for recovering Pd(II) from acidic solutions (Xie et al., 2020).

Glutaraldehyde-crosslinked polyethyleneimine (GLA-PEI) in algal biomass beads (AB/PEI) were prepared by Wang et al. and its sorption capacity for Pd(II) and Pt(IV) were studied (S. Wang et al., 2017). Sargin et al. reported synthesis of palladium supported on chitosan-carbon nanotube and its application in catalytic reduction of compounds containing nitro group (4-nitrophenol, 2-nitroaniline, 4-nitro-o-phenylenediamine and 2,4-dinitrophenol) and in degradation of dyes (Congo red, Methyl red, Methyl orange and Methylene blue) as well as for the synthesis of biaryls by Suzuki coupling reaction (Sargin et al., 2020).

Numerous covalent crosslinking agents are reported such as Glutaraldehyde, Epichlorohydrin, Glyoxal, Trimethyl propane triglycidyl ether, Ethylene glycol and diglycidyl ether (Józwiak et al., 2017).

Mincke et al., developed three Chitosan derivatives namely 1,10-phenanthroline-2,9-dicarbaldehyde cross-linked chitosan (Ch-PDC), [2,2'-bipyridine]-5,5'-dicarbaldehyde cross-linked chitosan (Ch-BPDC) and glutaraldehyde cross-linked chitosan grafted with 8-hydroxyquinoline-2-carbaldehyde (Ch-GA-HQC), and were employed for Pd(II) and Pt(IV) recovery from acidic solutions (Mincke et al., 2019). Ruiz et al., used glutaraldehyde as cross-linking agent to crosslink chitosan to study palladium recovery in acidic medium (Ruiz et al., 2000).

Nagireddi et al. prepared glutaraldehyde cross-linked chitosan and used for recovery of Pd from ELP solution. (Nagireddi et al., 2017). Gupta et al. have used glyoxal and glutaraldehyde cross linked chitosan for controlled drug delivery and had observed that glyoxal cross linked chitosan had better stability and efficiency (Gupta & Jabrail, 2006). Chitosan-glyoxal has been used as adsorbent for reactive and acid dyes at pH 3 (Yang et al., 2005) and chitosan cross linked with glyoxal loaded with palladium has been studied as a catalyst for Suzuki coupling reactions (T. Baran, 2016). Glyoxal is a polysaccharide containing two aldehyde groups. Cross linking involves either Schiff's base formation between the aldehyde groups of glyoxal and the free amino groups of chitosan or acetal formation between the aldehyde groups of glyoxal and the

hydroxyl groups of the glucosamine units of chitosan (Yang et al., 2005; Kaczmarek-Szczepanska et al., 2021).

However, Chitosan-glyoxal has not been studied as adsorbent for Pd. Chitosan-glyoxal supported Pd has not been reported as environment catalyst for catalytic reduction of dyes and toxic pollutants like Nitrophenol. Though Pd has been recovered from several environmental matrices using a wide range of adsorbents its valorization has not been demonstrated by researchers.

This work was directed towards investigating the Pd(II) adsorption characteristics on Glyoxal crosslinked chitosan (GCC) using synthetic electroless plating (ELP) solutions. The chitosan derivative GCC and Pd@GCC were characterized by various analytical techniques like Scanning Electron Microscopy, High Resolution Transmission Electron Microscopy, Energy Dispersive X-ray Spectroscopy, Fourier Transform Infrared Spectroscopy, Thermogravimetry, X-ray Photoelectron Spectroscopy, X-ray Absorption Near Edge Spectroscopy and X-Ray Diffraction techniques. Further Pd@GCC was valorized for multifarious applications such as C-C coupling reactions in mild conditions, catalytic dye reduction and nitrophenol reduction and sustainability of the catalyst was tested.

4.2. Materials and method

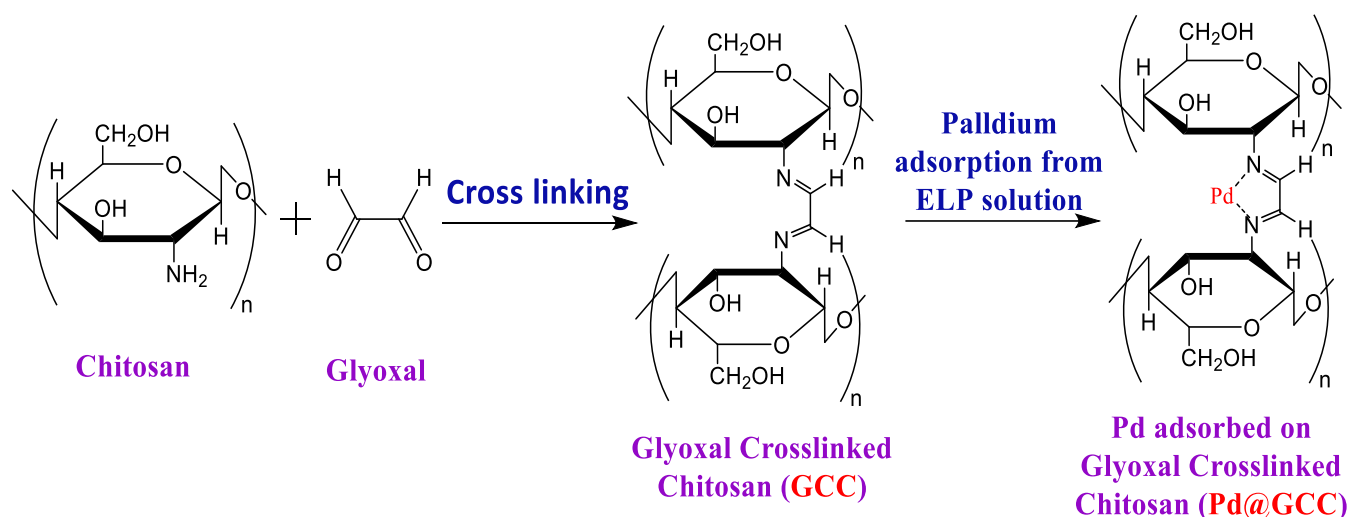
4.2.1. Materials

All chemicals were purchased as reagent grade from commercial suppliers and were used without further purification. Chitosan (from crab shells, 75-85% deacetylated of mean molecular weight ~190,000–310,000 Da) was purchased from Sigma-Aldrich. The synthesized materials were first dried in oven at 100°C and then used for further analysis.

4.2.2. Preparation of Glyoxal crosslinked chitosan derivative (GCC)

Firstly, 0.1 g chitosan was dissolved in 10 mL of water containing 0.1 mL acetic acid and stirred for 2-3 hours till homogeneous solution is obtained. Subsequently, 2 mL of glyoxal was added dropwise to chitosan solution and continued stirring for 1 hour for better mixing. The pH of the reaction mixture was then adjusted to 6-7 using 0.2 N NaOH which resulted in a yellowish–orange gel. The obtained gel was filtered and washed several times with

conductivity water followed by acetone and dried in vacuum oven at $\sim 100^{\circ}\text{C}$ for 9-10 h. The dried product was ground into fine powder by using mortar and pestle followed by washing in a soxhlet extractor with methanol for 24 h with the final product dried and used for Pd(II) adsorption study (Schematic 4.1).



Scheme 4.1: Schematic diagram of synthesis of Pd@GCC

4.2.3. Preparation of synthetic 50 ppm ELP solutions

Table 4.1 summarizes the composition of synthetic ELP solution used for batch adsorption studies. Along with Pd precursors, the synthetic ELP solution consists of Na_2EDTA stabilizer, Cetyl trimethylammonium bromide (CTAB) cationic surfactant and liquor ammonia.

Component's Name	Pd(II) concentration (in ppm) in solution					
	50	100	200	300	400	500
PdCl_2 (mg/L)	83.31	166.63	333.27	499.90	666.54	833.17
Na_2EDTA (g/L)	1.39					
NH_3 solution (25%), (mL/L)	10.33					
CTAB, (mg/L)	/335					

Table 4.1: Concentration of components in ELP solution

Stock Pd (II) solutions were prepared by dissolving 8.3 mg of PdCl₂ in 50 mL conductivity water. For complete dissolution of Pd(II), 1 mL of concentrated HCl was added and stirred for about half an hour. Subsequently, 0.13 mg Na₂EDTA and 33.5 mg CTAB (cationic surfactant) were added to the Pd(II) solution and kept for stirring on a magnetic stirrer till a clear solution was obtained. The pH was maintained between 6.0-7.5 using ammonia and the solution was made upto 100 mL and stirred till the resulting solution became colorless (Nagireddi et al., 2017)

4.2.4. Pd(II) adsorption experiments (Pd@GCC)

a) Optimization of Adsorbent dosage

A series of solutions containing 10 mL of 50ppm of Pd(II) solution with varying amounts (0.1-0.5g) of GCC were taken in polypropylene conical flasks and were agitated at 250 rpm in an orbital shaker for 3h at room temperature. After 3h, the solution was filtered through Whatman filter paper No. 1, and filtrate was analysed for unadsorbed Pd(II) using AAS spectrometer.

b) Optimization of Time

Synthetic ELP solutions containing 10 mL of 50 ppm Pd (II) were taken in 6 different conical flasks to which 0.2 g of GCC was added and the mixture was agitated in an orbital shaker at room temperature for different time intervals ranging from 30 to 180 minutes. The unabsorbed palladium was determined by AAS after filtering the solution.

c) Optimization of pH

Batch adsorption studies for the study of effect of pH was performed by setting pH 1-10 of 50 ppm Pd(II) solutions and were agitated with 0.2 g of GCC at 250 rpm at room temperature in an orbital shaker for 2 h. The solutions were filtered and collected for AAS analysis.

4.2.5. Suzuki coupling reaction using Pd@GCC

To a 25 mL round bottomed flask, 1.59 mmol Aryl halide, 1.59 mmol Phenylboronic acid, 3.18 mmol K₂CO₃, 3 mg Pd@GCC and 10 mL H₂O were added. The reaction mixture was heated to 100 °C in an oil bath and stirred for 10 to 24 h depending on the aryl halides used. The progress of the reaction was monitored by TLC. After completion of the reaction, the reaction mixture was cooled to room temperature and the product was extracted with 5mL ethyl acetate three times (3*5 mL). The catalyst was separated by filtration. The ethyl acetate phase was

collected, dried with Na_2SO_4 and the solvent was then removed under reduced pressure to get the crude product. Samples were analyzed by GC-MS and NMR.

To test the recyclability of Pd@GCC catalyst, after each cycle catalyst was separated, washed twice with 10 mL of 1:1 ethyl acetate:water and dried it in an oven at 100 °C for 5 h. The recovered catalyst could be used for the next cycle.

4.2.6. p-Nitrophenol reduction using Pd@GCC

In a 50 mL conical flask, 10 mL of 10 ppm p-NP solution, 4 mg NaBH_4 and 1 mg of catalyst were added at room temperature (30-35°C). The solutions were mixed by gentle shaking before each measurement. The reduction reaction was monitored by measuring the absorbance of the solution at different time intervals using UV-Vis absorption spectrophotometer.

The reusability of Pd@GCC was tested by collecting the catalyst after filtration, and washed twice with 10 mL conductivity water, dried in an oven at 100 °C for 3-4 h before the next cycle of the experiment.

4.2.7. Procedure for reduction of dyes using Pd@GCC

The reduction of dyes MB, MG, CV, R6G using sodium borohydride in the presence of 1 mg Pd@GCC was carried out at 30-35°C. A known amount of NaBH_4 was mixed with 10 mL of 5 ppm dye solution followed by the addition of 1 mg Pd@GCC. The decolorisation of the dyes was monitored by UV-Vis spectroscopy at 2 min intervals.

The reusability of Pd@GCC was tested by separating the catalyst by filtration, washed twice with 10 mL conductivity water followed by 5 mL acetone and placed in an oven to dry for 3-4 h before next cycle of the experiment.

4.2.8. Characterization of Pd@gGCC

The structural and morphological properties of GCC and Pd@GCC were analyzed by using XRD, SEM, EDX, HRTEM, XPS, HRTEM and XANES techniques as described in chapter 2 section 2.2.6.

Pd k-Edge XANES analysis

Samples (pellet) were prepared by grinding it in a mortar and pestle and pressed under high pressure under vacuum. Pd K-edge XANES experiments were performed in the emission mode, at the beamline BL12, INDUS-2 of the RRCAT Facility, Indore.

Determination of Palladium amount in mother liquor after adsorption by AAS

After completion of adsorption, the solution was filtered using Whatman filter paper no. 40 and the filtrate analysed by Thermo Electron corporation, S series, AAS spectrophotometer.

The palladium content in the catalyst and leaching study was performed by using PerkinElmer ICP-MS, NexION 2000 spectrometer by adapting the method described in chapter 3 section 3.2.8.

GC-MS spectra of crude products obtained after coupling reaction were recorded on Thermo fisher trace ultraGC model. NMR Spectrums of column purified Biphenyl products were recorded on Bruker Avance III spectrometer operating at 600 MHz in CDCl₃ solvent using procedure described in chapter 3 section 3.2.8.

4.3. Result and discussion**4.3.1. Adsorption of palladium from ELP solution**

The efficacy of GCC for palladium adsorption from electroless plating solution was investigated. The Pd(II) adsorption as a function of amount of adsorbent and time revealed the optimal values to be 0.2 g and 120 min. respectively (Figure 4.1(A &B)) wherein maximum adsorption occurred in the first 30 minutes. The adsorption of Pd(II) (Figure 4.1C) was observed to be equally effective over the entire pH range of 1-10 studied. Kinetic study of the adsorption of Pd from ELP solution was done. As seen from the plot of t/q_t against time (Figure 4.1D), the adsorption follows pseudo second order kinetics with a regression coefficient of 0.9979.

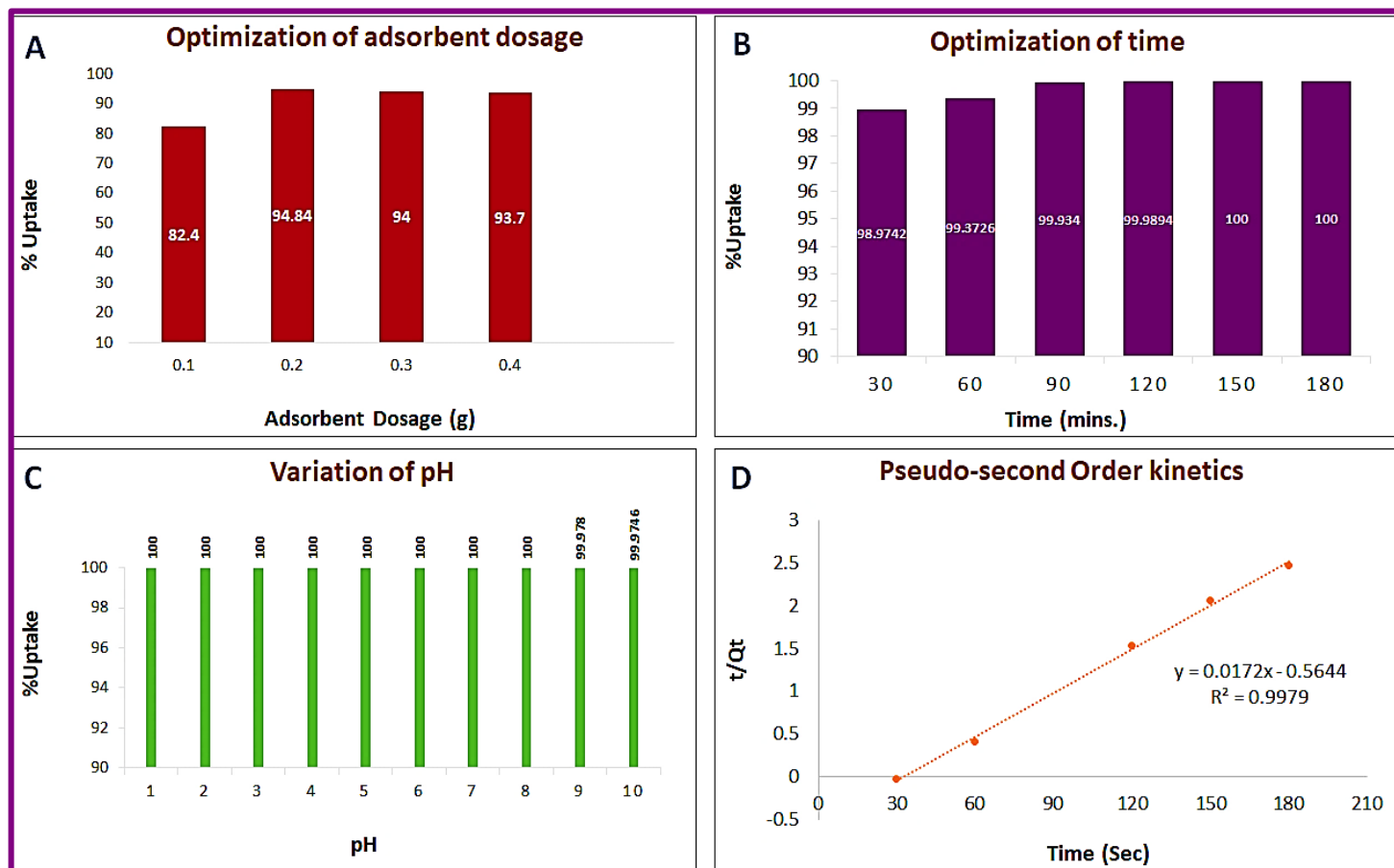


Figure 4.1: Optimization of Adsorption of Palladium from ELP solution

4.3.2. UV-Vis spectral analysis of Pd@GCC

Figure 4.2 shows the UV Vis absorption spectra of GCC and Pd@GCC. Pd@GCC exhibited a small band in UV region, around 280 nm attributed to Pd(0) and a peak around 390 nm attributed to Pd(II) (Larios-Rodríguez et al., 2013; Nemamcha et al., 2006).

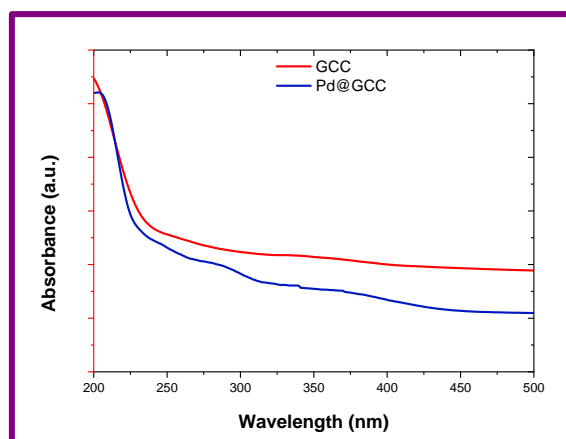


Figure 4.2: UV-vis spectra of GCC, Pd@GCC and Pd@GCC-r

4.3.3. FTIR spectral analysis

FTIR spectra for Chitosan, GCC and Pd@GCC are presented in Figure 4.3. FTIR spectrum of pristine chitosan exhibited characteristic bands of chitosan which included a broad band at 3415 cm^{-1} (N-H and O-H stretching), 1655 cm^{-1} (NH_2 bending) and 1030 cm^{-1} (C-O-C stretching) (Nate et al., 2018). The bands at 1561 and 1655 cm^{-1} were attributed to amide II and amide I groups of chitosan respectively. The stretching vibration peaks of C-N were observed at 1030 and 1075 cm^{-1} . In GCC a new peak was observed at 1644 cm^{-1} indicative of the formation of imine group due to cross linking of glyoxal with chitosan (T. Baran, 2016).

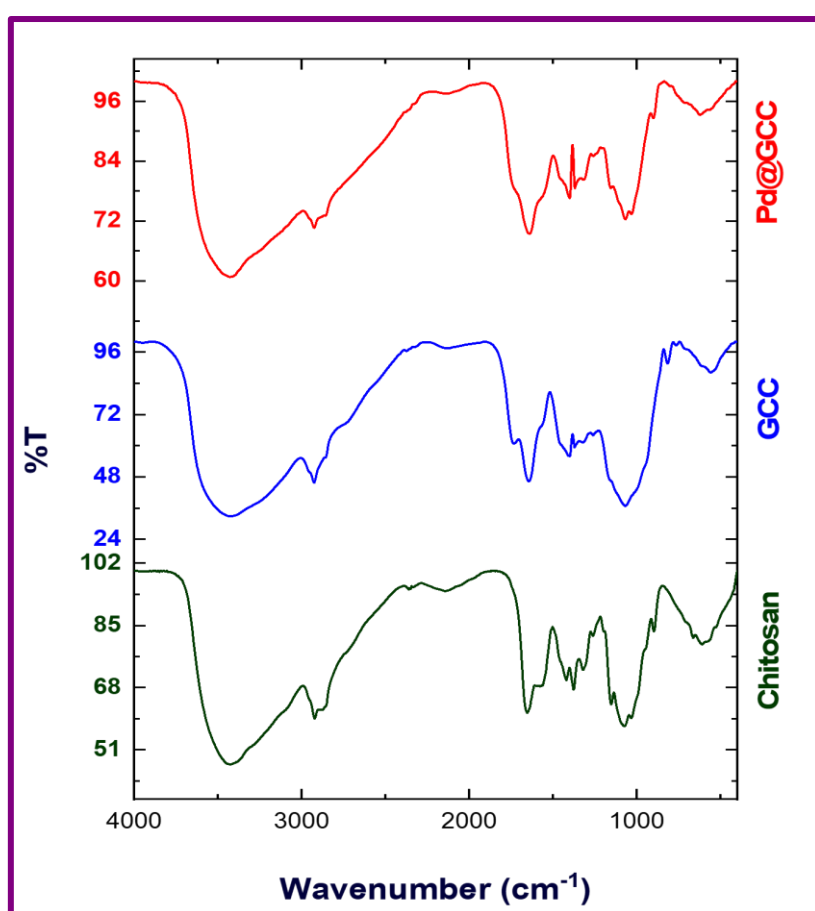


Figure 4.3: FTIR spectra of GCC and Pd@GCC

In addition, the N-H and O-H stretching vibrations were observed at 3429 cm^{-1} , the CH_3 symmetric stretch at 2925 cm^{-1} , C-N stretching vibration at 1400 cm^{-1} , CH_2 stretching bands at $\sim 1400\text{ cm}^{-1}$, C-OH stretching vibration at 1068 cm^{-1} and the CH_3 bending vibration at 1322 cm^{-1} for GCC (Gupta & Jabrail, 2006; Yang et al., 2005). After the adsorption of Pd onto GCC, peaks were found to be slightly shifted. This is indicative of the successful adsorption of Pd

onto GCC. A new peak was observed in Pd@GCC at 621 cm^{-1} , attributed to Pd-O bond representing the interaction of Pd with the surface of GCC (Anjum et al., 2020).

4.3.4. SEM-EDX

Surface morphology of GCC before and after adsorption of Pd were characterized by SEM. The morphology GCC was observed to be non-porous (Figure 4.4A) with homogeneous cross linking. It was also observed that GCC became shiny after Pd (II) adsorption (Figure 4.4B).

EDX analysis of Pd (II) loaded GCC obtained revealed Pd weight% to be about 3.56% in Pd@GCC (Figure 4.4C). The EDX also confirmed the presence of O (69.12 wt%), N (15.49 wt%) and C (11.83 wt%) in Pd@GCC. Pd content were also analyzed by Inductively Coupled Plasma-Mass Spectrometry (ICP-MS). The results showed that the Pd content of the final product is 0.24 wt% for Pd@GCC

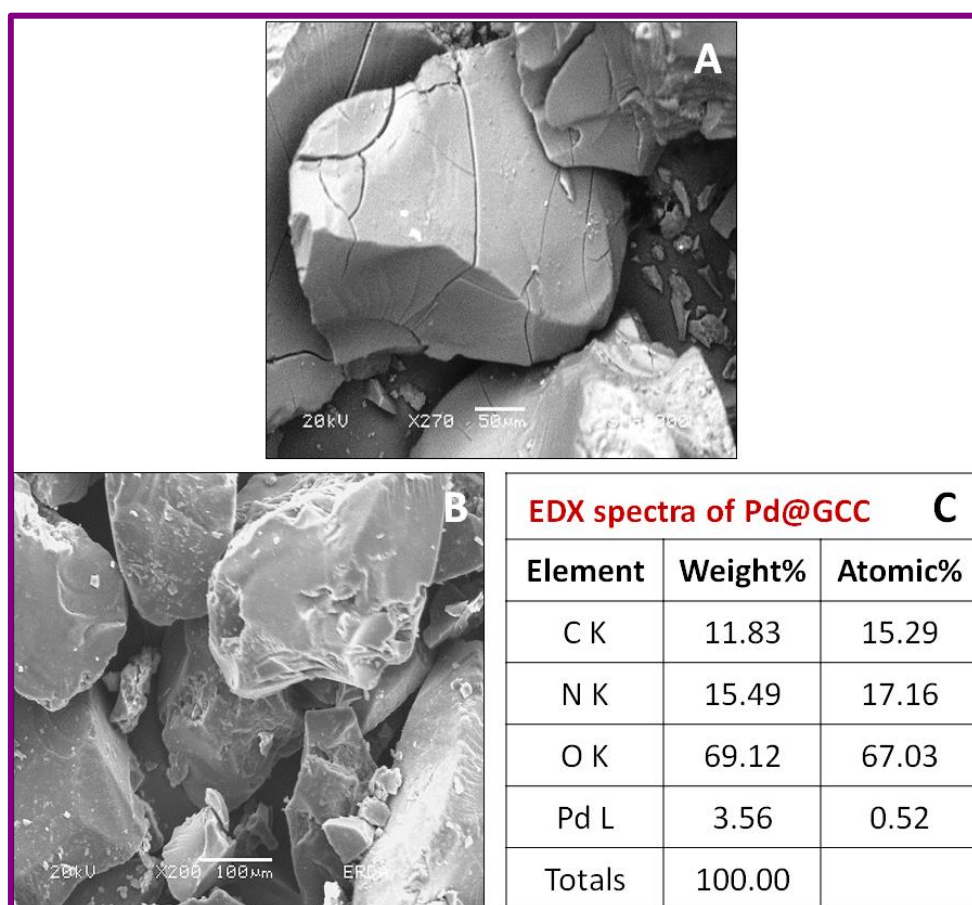


Figure 4.4: (A) SEM image of GCC, (B) SEM image of Pd@GCC, (C) EDX of Pd@GCC, (D,E) HRTEM image of Pd@GCC, (F) SAED pattern of Pd@GCC

4.3.5. HRTEM and SAED

The HRTEM images of Pd@GCC (Figure 4.5A,B) clearly revealed fivefold twinned icosahedron shaped palladium particles dispersed in GCC. Particle size of palladium (Pd@GCC) was in the range of 24–30 nm. Lattice fringes (Figure 4.5B) with lattice spacing 0.205 nm characteristic of (200) plane of fcc Pd were observed. Lattice fringes observed with lattice spacing of 0.221 nm were attributed to (110) plane of PdO (C. Wang et al., 2015). The SAED pattern (Figure 4.5C) corresponded to (220) plane of Pd and (103) plane of PdO.

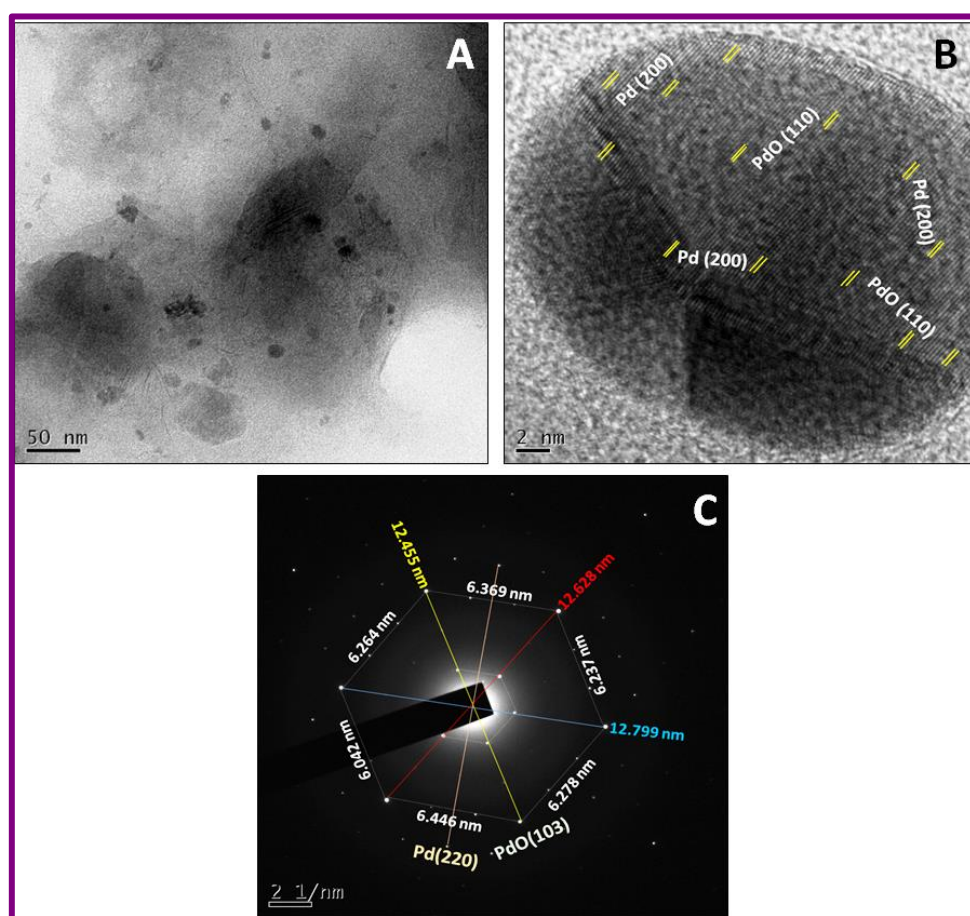


Figure 4.5: (A) TEM image of Pd@GCC (B) HRTEM image of Pd@GCC, (C) SAED pattern of Pd@GCC

4.3.6. PXRD Analysis

X-ray diffraction (XRD) patterns recorded for GCC and Pd@GCC are presented in Figure 4.6. chitosan show two strong characteristics peaks at ~ 10 and 20° with high degree of crystallinity

(Qi et al., 2004). In GCC, The characteristic peaks of chitosan at 20° disappeared (Govindan et al., 2012), and a broad peak centered at $2\theta = 23^\circ$ appeared.

This difference in XRD patterns between chitosan and GCC should be attributed to the cross-linking reaction between chitosan and glyoxal wherein the crystallinity of chitosan decreased after crosslinking with glyoxal (T. Baran, 2016). This could be attributed to the substitution of hydroxyl and amino groups resulting in deformation of the hydrogen bonds in original chitosan which efficiently destroyed the regularity of the packing of the original chitosan chains and resulted in the formation of amorphous GCC.

The planes that corresponded to GCC were relatively suppressed due to crystallinity of palladium in the XRD pattern of Pd@GCC while peaks at 39.6° , and 46.7° corresponded to (111) and (200) planes of palladium (JCPDS # 89-4897) (T. J. Wang et al., 2020) and the one at 33.9° attributed to (110) plane of PdO were observed (ICSD 00-043-1024). (N. Y. Baran et al., 2018; Walls et al., 2019).

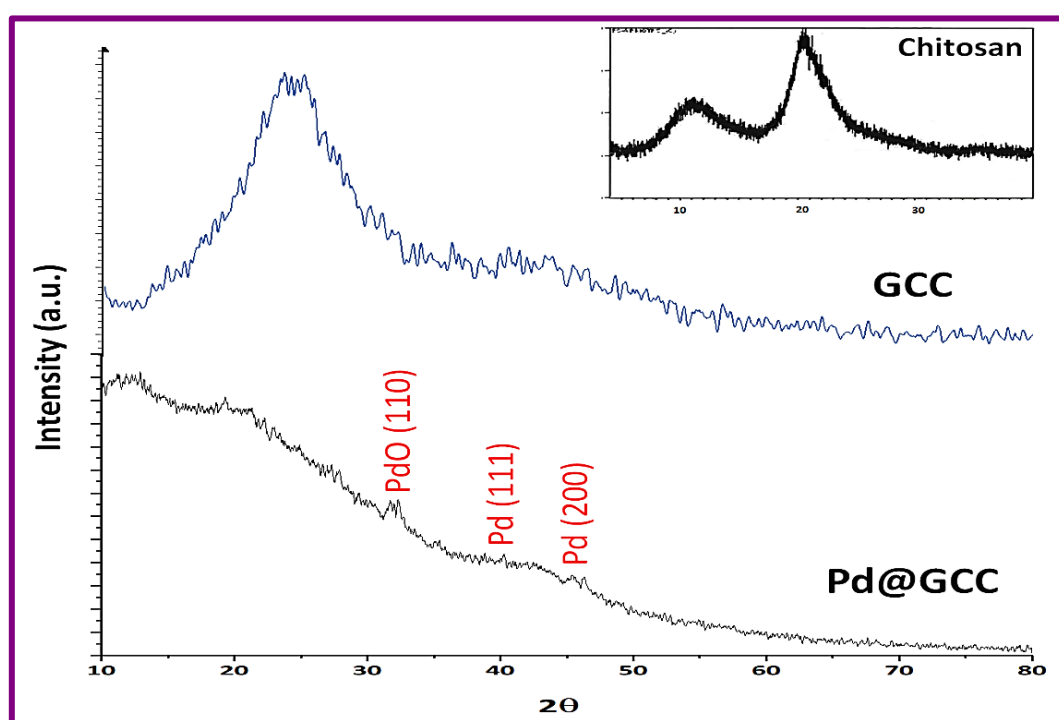


Figure 4.6: XRD pattern of Chitosan, GCC and Pd@GCC

4.3.7. XPS Analysis

XPS analysis of Pd@GCC was performed to understand the chemical binding states and composition of the samples.

In the region of 330–345 eV two well defined spin–orbit doublets of Pd 3d_{5/2} and Pd 3d_{3/2} with 5.2 eV spin orbit splitting (Figure 4.7B.) were observed. Pd XPS peaks observed at 335.05 and 340.25 eV were attributed to Pd (0) 3d_{5/2} and 3d_{3/2} spin orbit doublets. The Pd 3d_{5/2} and 3d_{3/2} peaks observed at 336.81 eV and 342.01 respectively were assigned to Pd²⁺ (Peuckert, 1985). Detailed XPS assignments are given in appendix (Table 4.A1-4.A3).

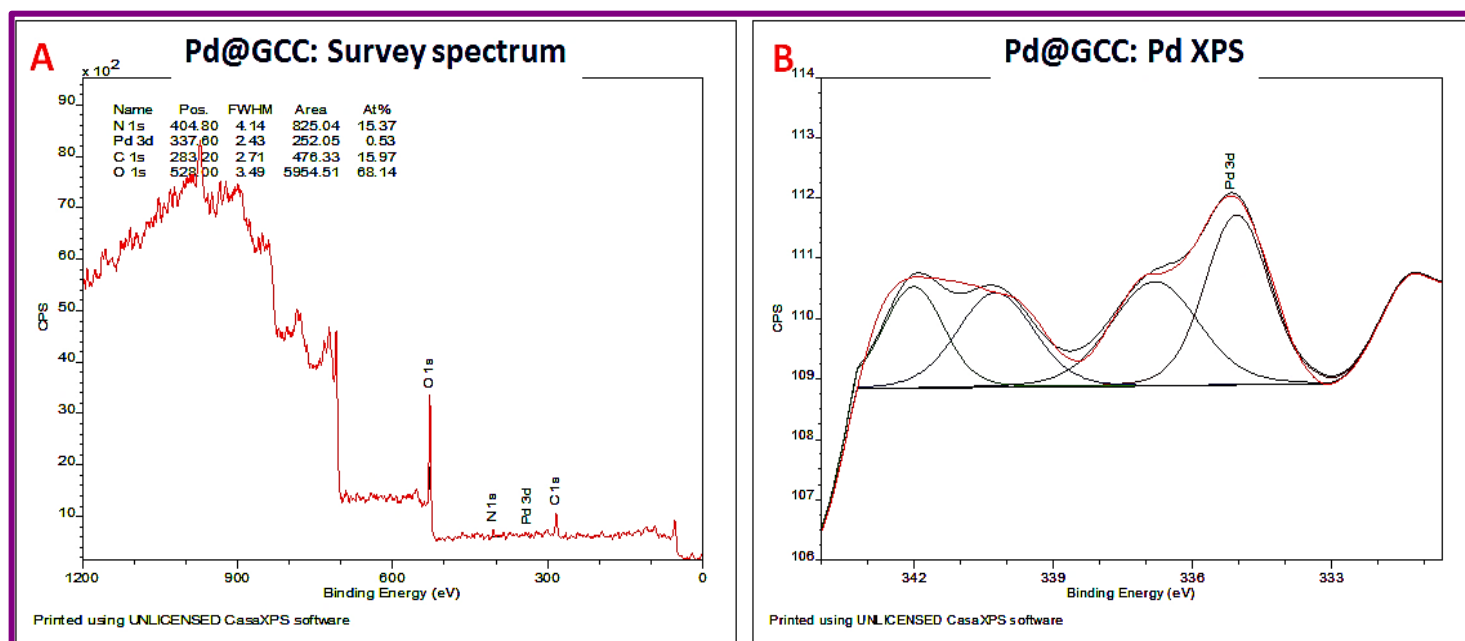


Figure 4.7: (A) XPS survey spectra of Pd@GCC, (B) Pd XPS spectra of Pd@GCC

4.3.8. TG-DTA Analysis

The TGA analysis of GCC and Pd@GCC (Figure 4.8(A&B)) was performed to understand the degradation profile. GCC exhibited, the first mass loss of 10.4% between 50°C and 150°C attributed to moisture vaporization. The second weight loss of about 49.6% which started at about 150 °C was attributed to the decomposition of chitosan. The total weight loss of GCC upto 750 °C was 67.1%. Similarly, the mass loss study of the Pd@GCC exhibited 69.64% total weight loss upto 750 °C.

4.3.9. XANES Analysis

The oxidation state of Pd in Pd@GCC was further studied through X-ray absorption near edge spectra (XANES) (Figure 4.8C). The Pd K-edge XANES spectra of Pd@GCC was compared with the spectrum of the reference metallic palladium. From the figure it is clear that the

Pd@GCC XANES spectra did not compare with Pd foil but resembled PdO (Keating et al., 2013)

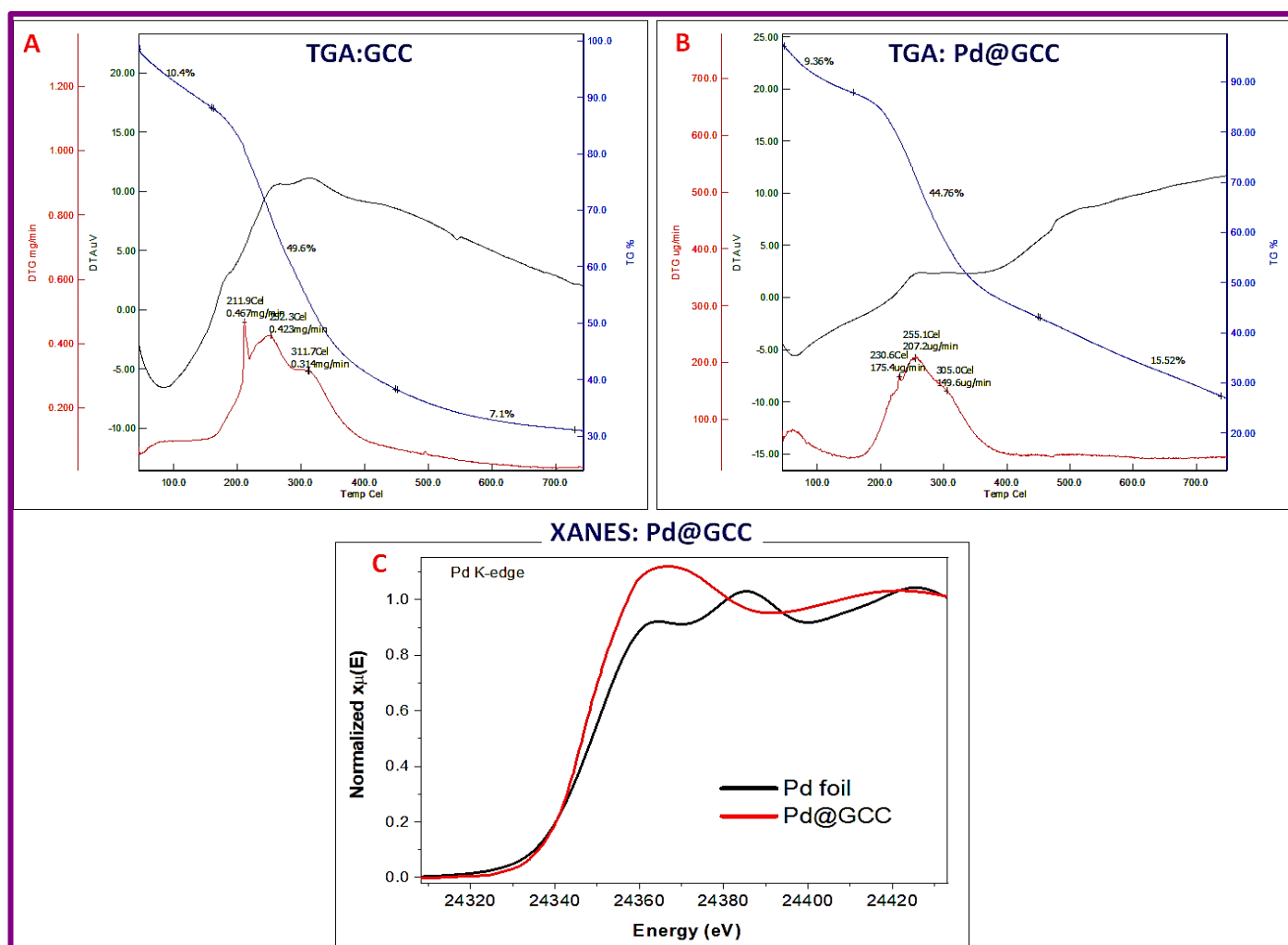


Figure 4.8: (A) Thermogram of GCC, (B) Thermogram of Pd@GCC, (C) Pd K edge XANES spectra of Pd@GCC

4.4. Catalytic performance studies

4.4.1. Suzuki coupling reaction in water catalysed by Pd@GCC

The catalytic potential of Pd@GCC was investigated for Suzuki coupling synthesis of biphenyls. The reaction between Iodobenzene and phenyl boronic acid was chosen as a model coupling reaction for the optimization of reaction conditions such as amount of the catalyst, temperature, time, nature of base system, amount of base and reaction duration. Initial runs of coupling reaction were carried out using 1 mg of catalyst and 1.59 mmol substrate at 100°C that led to a 74.82% yield of biphenyl after 12 h (Figure 4.A2). On increasing the catalyst dose

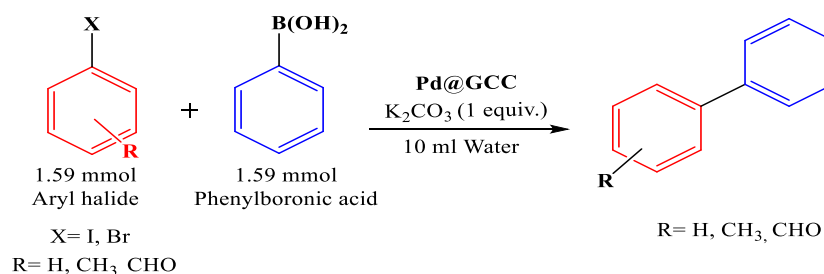
to 3 mg the reaction proceeded successfully (100% Yield) at 100°C. On performing the reaction at lower temperatures, it was observed that biphenyl yield was not quantitative (100°C, 99.9% yield; 30-35°C, 0% Yield; 60°C, 72.94% yield) (Figure 4.A3). The effect of different bases on the biphenyl yield was evaluated (NaOH, 0% yield; KOH, 18% yield; Na₂CO₃, 98% yield; K₂CO₃, 98.70% yield) (Figure 4.A4) indicating that the highest yield was achieved with K₂CO₃. The ideal reaction time for Suzuki coupling reactions catalyzed by Pd@GCC was determined to be 9 h.

After the optimization of reaction conditions for the Suzuki coupling reactions, the effect of different substituents such as electron-withdrawing and electron-donor on biphenyl yields was studied with Pd@GCC under optimal conditions. The influence of reactivity of aryl halides (I, Br and Cl) on the Suzuki reactions was further investigated. Excellent yields with high turnover number (1584.34) and high turnover frequency (176.03 h⁻¹) were obtained with Iodobenzene (Table 4.2, entry 1). Bromobenzene and Chlorobenzene also gave high reaction yields (Table 4.2, entries 6&7) but took longer time (9h for Iodobenzene; 10h for bromobenzene; 12h for Chlorobenzene), According to the entries seen in Table 4.1, reactivity order of the Aryl halide was found as R-I > R-Br > R-Cl.

Studies on the effect of the substituent revealed that electron-withdrawing group (-CHO) (Table 4.2 entries 4&5) on the substrate gave higher reaction yields than electron donor group (-CH₃) (Table 4.2 entries 2&3). It was also observed that para-substituted substrates were more active than ortho substituent on Aryl halide (N. Y. Baran et al., 2018; Yi et al., 2007).

Table 4.2: Suzuki coupling reaction catalysed by Pd@GCC in aqueous system

Reaction Condition: 1.59 mmol Aryl halide, 1.59 mmol Phenylboronic acid, 3mg catalyst, 2 mol equivalent K₂CO₃, 10 ml water



Sr. No.	X	R	Temperature (°C) & Time (hrs.)	GC-MS Yield (%)	Isolated Yield (%)
1	I	H	100 °C, 9 h	99.9	99.9

2	I	p-CH ₃	100°C, 12 h	80.72	80
3	I	o-CH ₃	100°C, 15 h	79.50	78.4
4	I	p-CHO	100°C, 14 h	97.82	96.5
5	I	o-CHO	100°C, 20 h.	96.28	95.8
6	Br	H	100°C, 10 h	99.1	99.0
7	Cl	H	100°C, 12 h	98.5	98.1

Recyclability of the catalyst

To study the recyclability of Pd@GCC at the end of the model Suzuki coupling reaction, the Pd catalyst was filtered and rinsed several times with water and acetone for regeneration of the catalyst. This process was repeated after completion of each run and the reusability of the Pd@GCC was tested under optimal reaction conditions. It was observed that Pd@GCC still could exhibit a 99.9% conversion upto four cycles. After the fourth cycle there was a 11% decrease in conversion that could be attributed to the gradual leaching of palladium analysed by ICP-MS (1st cycle: 1.51ppb Pd; 2nd cycle: 1.81ppb Pd; 3rd cycle: 3.19 ppb Pd; 4th cycle: 4.49 ppb Pd; 5th cycle: 23.22 ppb Pd). The structure of the recycled Pd catalyst (Pd@GCC) was investigated by using FTIR spectroscopy (Figure 4.9). The characteristic peaks of fresh Pd@GCC were retained in the recycled catalyst indicating that chemical structure Pd@GCC was preserved up to 4 cycles.

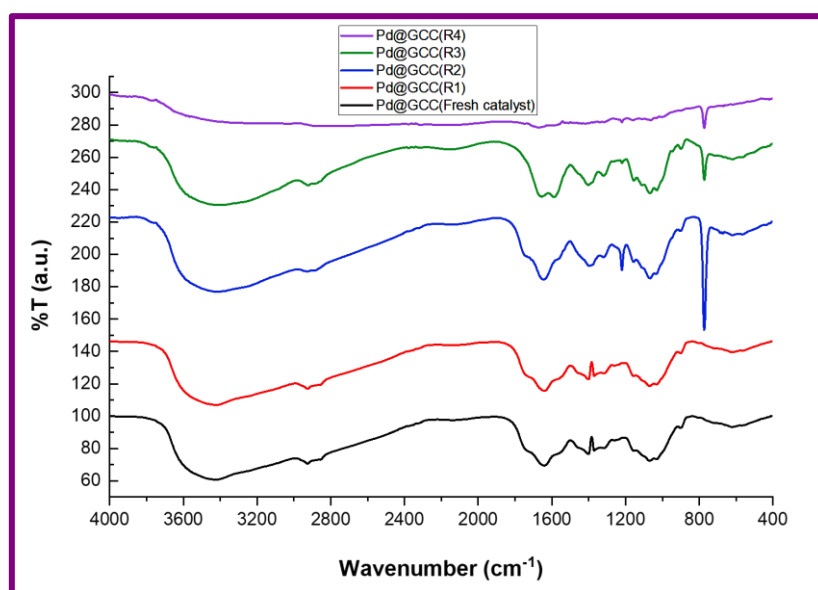


Figure 4.9: Overlay IR spectra of Recycled Pd@GCC catalyst

4.4.2. Catalytic reduction of p-NP in the presence of Pd@GCC

In order to determine the efficiency of the Pd@GCC for hydrogenation reactions, hydrogenation of p-Nitrophenol (p-NP) to p-Aminophenol (p-AP) was studied at room temperature using sodium borohydride as reducing agent and was monitored by using UV-Vis absorption spectroscopy. (Figure 4.10)

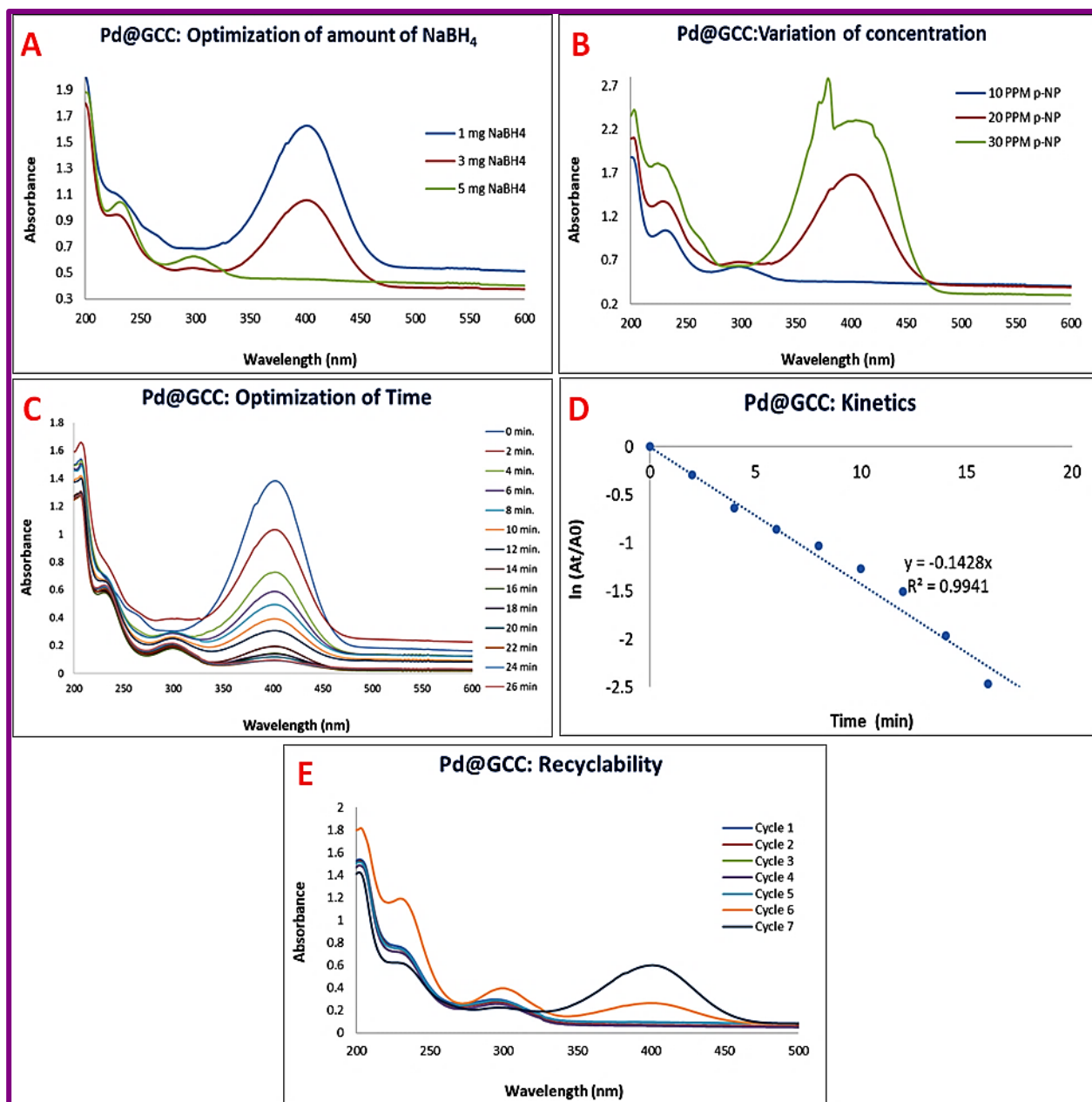


Figure 4.10: Reduction of p-NP catalyzed by Pd@GCC

The product p-AP obtained is a precursor for the synthesis of a drug molecule paracetamol, thus signifying the valorization of a potential hazardous chemical as well as recovery palladium

from ELP solution. The original yellow aqueous p-NP solution exhibited an absorption maximum at 320 nm. After addition of NaBH₄, the color of p-NP was intensified to dark yellow because of the formation of p-nitrophenolate ion and λ_{max} was red shifted to 402 nm. After addition of the catalyst, color of the solution faded and turned to colorless on completion of the reduction of p-NP. The absorption peak at 402 nm was gradually decreased and new peak appeared at 305 nm due to the formation of p-AP (Ghanbari et al., 2017).

Figure 4.10C shows the UV-Vis spectra of the reduction of p-NP at the interval of every 2 min. from the start of the reaction. Figure 4.9D shows the plot of $\ln(A_t/A_0)$ versus time for the kinetic study of the reaction. The plot indicated that the reaction followed first order kinetics (Figure 4.10D) with respect to reduction of p-NP as concentration of NaBH₄ was high during the reaction and changed negligibly during the course of the reaction (Baghbmidi et al., 2018; T. Baran & Nasrollahzadeh, 2019).

The rate constant was determined to be 0.1428 min⁻¹ for Pd@GCC. Figure 4.10E shows representative recyclability data of Pd@GCC, wherein 100% reduction was achieved in 26 min, in the first cycle while the 5th cycle required 30 min to accomplish the reduction process.

4.4.3. Reduction of dyes catalysed by Pd@GCC

The catalytic efficiency of the prepared Pd@GCC catalyst was studied for the catalytic reduction of Methylene blue (MB), Malachite green (MG), Rhodamine 6g (R6g), and Crystal violet (CV). The progress of reaction was monitored by UV-Vis spectrophotometer and also visual observation of complete disappearance of color of dyes. Figure 4.11A shows that Pd@GCC was efficient in the reduction of MB, MG, CV and Rh6G by NaBH₄. MG reacted faster and degraded within seconds (Figure 4.11B).

The absorption peak at 664 nm for MB was found to decrease gradually with the increase in time indicating the slow degradation process of the dye (Figure 4.11C). The linear correlation between $\ln(A_t/A_0)$ versus reduction time in minutes (Figure 4.11D) indicated that the reduction followed first-order reaction kinetics with respect to concentration of MB as the concentration of NaBH₄ was relatively higher than that of MB. The rate constant was calculated from the slope of the graph and was found to be 0.80 min⁻¹ while the rate constants were 0.803 min⁻¹ and 0.348 min⁻¹ for CV and Rh6G respectively.

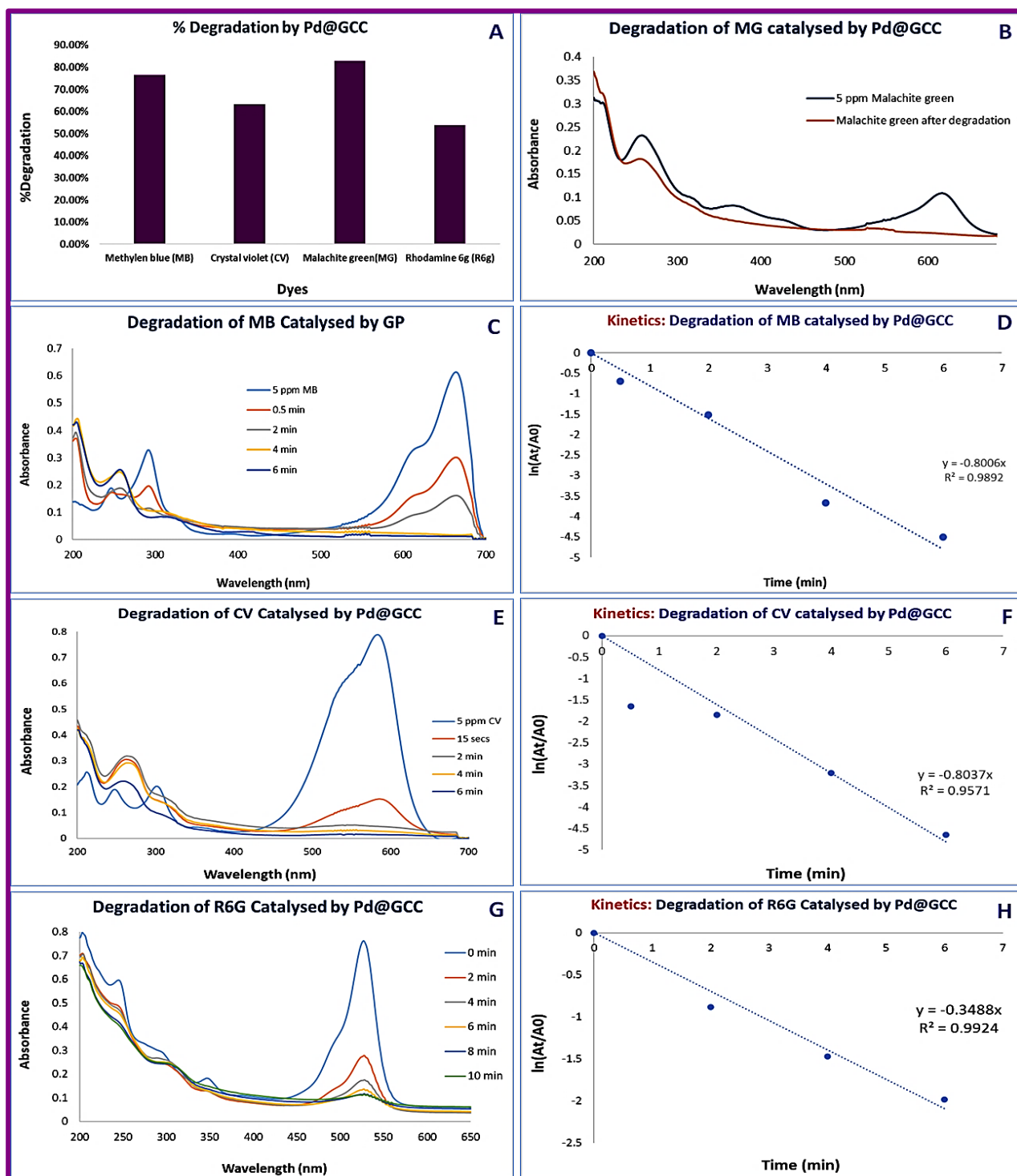


Figure 4.11: Degradation of Dyes (Malachite green, Methylene blue, Crystal violet, Rhodamine 6g) catalyzed by Pd@GCC

Influence of pH in dye degradation was studied in acidic, neutral and alkaline pH conditions. It was observed that at pH 7, the degradation of methylene blue was the highest, reaching 96.97%. while at pH 4 and 10, 55% and 58% degradation respectively was observed (Teng et

al., 2020). Recyclability of the catalysts were tested with MB and it was observed that Pd@GCC was recycled without loss in catalytic efficiency upto 8 cycles.

Pd@GCC showed much higher recyclability for the p-NP reduction and MB degradation than for Suzuki coupling. This could be due to the higher reaction temperature (100 °C) required for Suzuki coupling reaction. Perhaps, a change of the coordination sites of Pd on the support during reaction and work-up is responsible for this effect (Martina et al., 2011).

4.4. Conclusion

The prepared Glyoxal Cross Linked Chitosan (GCC) was well characterized and used for adsorption of Pd from electroless plating solution (Pd@GCC). Pd@GCC was valorized as a catalyst for the Suzuki coupling reaction, dye degradation and p-NP reduction. From these studies it was proven that, GCC effectively interacts with palladium, thereby leading to excellent palladium recovery and its reusability in catalytic applications. Furthermore, the reduction of Pd@GCC and the catalytic applications were carried out in aqueous medium, offering an environmentally benign methodology.

4.5. References

- Anjum, F., Gul, S., Khan, M. I., & Khan, M. A. (2020). Efficient synthesis of palladium nanoparticles using guar gum as stabilizer their applications as catalyst in reduction reactions and degradation of azo dyes. *Green Process Synth*, 9(1), 63–76. <https://doi.org/10.1515/gps-2020-0008>
- Baghbamidi, S. E., Hassankhani, A., Sanchooli, E., & Sadeghzadeh, S. M. (2018). The reduction of 4-nitrophenol and 2-nitroaniline by palladium catalyst based on a KCC-1/IL in aqueous solution. *Appl. Organometal. Chem.*, 32(4), 4251. <https://doi.org/10.1002/aoc.4251>
- Baran, N. Y., Baran, T., & Mente, A. (2018). Production of novel palladium nanocatalyst stabilized with sustainable chitosan/cellulose composite and its catalytic performance in Suzuki- Miyaura coupling reactions. *Carbohydrate Polymers*, 181, 596–604. <https://doi.org/10.1016/j.carbpol.2017.11.107>
- Baran, T. (2016). New Chitosan-Glyoxal Beads Supported Pd(II) Catalyst: Synthesis, Characterization and Application in Suzuki Coupling Reactions. *J. Biol. & Chem.*, 44(3), 307–315. <https://doi.org/10.15671/HJBC.20164420573>
- Baran, T., & Nasrollahzadeh, M. (2019). Facile synthesis of palladium nanoparticles immobilized on magnetic biodegradable microcapsules used as effective and recyclable catalyst in Suzuki-Miyaura reaction and p -nitrophenol reduction. *Carbohydrate Polymers*, 222, 115029. <https://doi.org/10.1016/j.carbpol.2019.115029>
- Begum, S., Yuhana, N. Y., Saleh, N. M., Kamarudin, N. H. N., & Sulong, A. B. (2021).

- Review of chitosan composite as a heavy metal adsorbent : Material preparation and properties. *Carbohydrate Polymers*, 259, 117613.
<https://doi.org/10.1016/j.carbpol.2021.117613>
- Buekenhoudt, A., Kovalevsky, A., Luyten, I. J., & Snijkers, F. (2010). 1 . 11 Basic Aspects in Inorganic Membrane Preparation. *Comprehensive Membrane Science and Engineering*, 1, 217–252. <https://doi.org/10.1016/B978-0-08-093250-7.00011-6>
- Chang, X., Chen, D., & Jiao, X. (2008). Chitosan-Based Aerogels with High Adsorption Performance. *J. Phys. Chem. B*, 112(26), 7721–7725. <https://doi.org/10.1021/jp8011359>
- Cheng, Y. S., & Yeung, K. L. (2001). Effects of electroless plating chemistry on the synthesis of palladium membranes. *Journal of Membrane Science*, 182(1–2), 195–203.
[https://doi.org/10.1016/S0376-7388\(00\)00563-9](https://doi.org/10.1016/S0376-7388(00)00563-9)
- Ghanbari, N., Hoseini, S. J., & Bahrami, M. (2017). Ultrasonic assisted synthesis of palladium-nickel/iron oxide core-shell nanoalloys as effective catalyst for Suzuki-Miyaura and p -nitrophenol reduction reactions. *Ultrasonics - Sonochemistry*, 39, 467–477. <https://doi.org/10.1016/j.ultsonch.2017.05.015>
- Godlewska-Zyłkiewicz, B., Sawicka, S., & Karpinska, J. (2019). Removal of Platinum and Palladium from Wastewater by Means of Biosorption on Fungi *Aspergillus* sp. and Yeast *Saccharomyces* sp. *Water*, 11, 1522.
- Govindan, S., Nivethaa, E. A. K., Saravanan, R., Narayanan, V., & Stephen, A. (2012). Synthesis and characterization of Chitosan–Silver nanocomposite. *Applied Nanoscience*, 2, 299–303. <https://doi.org/10.1007/s13204-012-0109-5>
- Gupta, K. C., & Jabrail, F. H. (2006). Glutaraldehyde and glyoxal cross-linked chitosan microspheres for controlled delivery of centchroman. *Carbohydrate Research*, 341(6), 744–756. <https://doi.org/10.1016/j.carres.2006.02.003>
- HariPriyan, U., Gopinath, K. P., & Arun, J. (2022). Chitosan based nano adsorbents and its types for heavy metal removal : A mini review. *Materials Letters*, 312, 131670.
<https://doi.org/10.1016/j.matlet.2022.131670>
- Józwiak, T., Filipkowska, U., Szymczyk, P., Rodziewicz, J., & Mielcarek, A. (2017). Effect of ionic and covalent crosslinking agents on properties of chitosan beads and sorption effectiveness of Reactive Black 5 dye. *Reactive and Functional Polymers*, 114, 58–74.
<https://doi.org/10.1016/j.reactfunctpolym.2017.03.007>
- Kaczmarek-Szczepanska, B., Mazur, O., Michalska-Sionkowska, M., Łukowicz, K., & Osyczka, A. M. (2021). The Preparation and Characterization of Chitosan-Based Hydrogels Cross-Linked by Glyoxal. *Materials*, 14, 2449.
<https://doi.org/10.3390/ma14092449>
- Keating, J., Sankar, G., Hyde, T. I., Kohara, S., & Ohara, K. (2013). Elucidation of structure and nature of the PdO-Pd transformation using in situ PDF and XAS techniques. *Physical Chemistry Chemical Physics*, 15(22), 8555–8565.
<https://doi.org/10.1039/c3cp50600b>

- Larios-Rodríguez, E. A., Castellón-Barraza, F. F., Borbón-González, D. J., Herrera-Urbina, R., & Posada-Amarillas, A. (2013). Green-Chemical Synthesis of Monodisperse Au, Pd and Bimetallic (Core–Shell) Au–Pd, Pd–Au Nanoparticles. *Advanced Sciences, Engineering and Medicine*, 5, 1–8. <https://doi.org/10.1166/ asem.2013.1354>
- Lee, S. J., Yu, Y., Jung, H. J., Naik, S. S., Yeon, S., & Choi, M. Y. (2021). Efficient recovery of palladium nanoparticles from industrial wastewater and their catalytic activity toward reduction of 4-nitrophenol. *Chemosphere*, 262, 128358. <https://doi.org/10.1016/j. chemosphere.2020.128358>
- Leonhardt, S. E. S., Stolle, A., Ondruschka, B., Cravotto, G., Leo, C. De, Jandt, K. D., & Keller, T. F. (2010). Chitosan as a support for heterogeneous Pd catalysts in liquid phase catalysis. *Applied Catalysis A : General*, 379, 30–37. <https://doi.org/10.1016/j. apcata.2010.02.029>
- Martina, K., Leonhardt, S. E. S., Ondruschka, B., Curini, M., Binello, A., & Cravotto, G. (2011). In situ cross-linked chitosan Cu (I) or Pd (II) complexes as a versatile , eco-friendly recyclable solid catalyst. *Journal of Molecular Catalysis A : Chemical*, 334, 60–64. <https://doi.org/10.1016/j. molcata.2010.10.024>
- Mincke, S., Asere, T. G., Verheye, I., Folens, K., Bussche, F. Vanden, Lapeire, L., Verbeken, K., Voort, P. Van Der, Tessema, D. A., Fufa, F., Laing, G. Du, & Stevens, C. V. (2019). Functionalized chitosan adsorbents allow recovery of palladium and platinum from acidic aqueous solutions. *Green Chemistry*, 21, 2295–2306. <https://doi.org/10.1039/C9GC00166B>
- Nagarjuna, R., Sharma, S., Rajesh, N., & Ganesan, R. (2017). Effective Adsorption of Precious Metal Palladium over Polyethyleneimine-Functionalized Alumina Nanopowder and Its Reusability as a Catalyst for Energy and Environmental Applications. *ACS Omega*, 2, 4494–4504. <https://doi.org/10.1021/acsomega.7b00431>
- Nagireddi, S., Golder, A. K., & Uppaluri, R. (2018). Role of protonation and functional groups in Pd (II) recovery and reuse characteristics of commercial anion exchange resin-synthetic electroless plating solution systems. *Journal of Water Process Engineering*, 22, 227–238. <https://doi.org/10.1016/j. jwpe.2018.02.008>
- Nagireddi, S., Katiyar, V., & Uppaluri, R. (2017). Pd(II) adsorption characteristics of glutaraldehyde cross-linked chitosan copolymer resin. *International Journal of Biological Macromolecules*, 94(A), 72–84. <https://doi.org/10.1016/j. ijbiomac.2016.09.088>
- Nate, Z., Moloto, M. J., Mubiayi, P. K., & Sibiya, P. N. (2018). Green synthesis of chitosan capped silver nanoparticles and their antimicrobial activity. *MRS Advances*, 3(42–43), 2505–2517. <https://doi.org/10.1557/adv.2018.3>
- Nemamcha, A., Rehspringer, J., & Khatmi, D. (2006). Synthesis of Palladium Nanoparticles by Sonochemical Reduction of Palladium (II) Nitrate in Aqueous Solution. *J. Phys. Chem. B*, 110, 383–387. <https://doi.org/10.1021/jp0535801>
- Parajuli, D., & Hirota, K. (2009). Recovery of palladium using chemically modified cedar

- wood powder. *Journal of Colloid and Interface Science*, 338, 371–375. <https://doi.org/10.1016/j.jcis.2009.06.043>
- Peuckert, M. (1985). XPS study on surface and bulk palladium oxide, its thermal stability, and a comparison with other noble metal oxides. *Journal of Physical Chemistry*, 89, 2481–2486. <https://doi.org/10.1021/j100258a012>
- Qi, L., Xu, Z., Jiang, X., Hu, C., & Zou, X. (2004). Preparation and antibacterial activity of chitosan nanoparticles. *Carbohydrate Research*, 339, 2693–2700. <https://doi.org/10.1016/j.carres.2004.09.007>
- Ruiz, M., Sastre, A. M., & Guibal, E. (2000). Palladium sorption on glutaraldehyde-crosslinked chitosan. *Reactive & Functional Polymers*, 45(3), 155–173. [https://doi.org/10.1016/S1381-5148\(00\)00019-5](https://doi.org/10.1016/S1381-5148(00)00019-5)
- Sahin, M., & Gubbuk, I. H. (2022). Green synthesis of palladium nanoparticles and investigation of their catalytic activity for methylene blue, methyl orange and rhodamine B degradation by sodium borohydride. *Reaction Kinetics, Mechanisms and Catalysis*, 135, 999–1010. <https://doi.org/10.1007/s11144-022-02185-y>
- Sargin, I., Baran, T., & Arslan, G. (2020). Separation and Purification Technology Environmental remediation by chitosan-carbon nanotube supported palladium nanoparticles : Conversion of toxic nitroarenes into aromatic amines , degradation of dye pollutants and green synthesis of biaryls. *Separation and Purification Technology*, 247, 116987. <https://doi.org/10.1016/j.seppur.2020.116987>
- Shari, H., Ashtiani, F. Z., & Soleimani, M. (2012). Adsorption of palladium and platinum from aqueous solutions by chitosan and activated carbon coated with chitosan. *Asia-Pac. J. Chem. Eng.*, 8(3), 384–395. <https://doi.org/10.1002/apj.1671>
- Teng, X., Li, J., Wang, Z., Wei, Z., Chen, C., Du, K., Zhao, C., Yanga, G., & Lid, Y. (2020). Performance and mechanism of methylene blue degradation by an electrochemical process. *RSC Adv.*, 10, 24712–24720. <https://doi.org/10.1039/d0ra03963b>
- Walls, J. M., Sagu, J. S., & Wijayantha, K. G. U. (2019). Microwave synthesised Pd–TiO₂ for photocatalytic ammonia production. *RSC Adv.*, 9, 6387–6394. <https://doi.org/10.1039/C8RA09762C>
- Wang, C., Yang, F., Yang, W., Ren, L., Zhang, Y., Jia, X., Zhang, L., & Li, Y. (2015). PdO nanoparticles enhancing the catalytic activity of Pd/carbon nanotubes for 4-nitrophenol reduction. *RSC Advances*, 5(35), 27526–27532. <https://doi.org/10.1039/C4RA16792A>
- Wang, S., Vincent, T., Roux, J., Faur, C., & Guibal, E. (2017). Pd(II) and Pt(IV) sorption using alginate and algal-based beads. *Chemical Engineering Journal*, 313, 567–579. <https://doi.org/10.1016/j.cej.2016.12.039>
- Wang, T. J., Li, F. M., Huang, H., Yin, S. W., Chen, P., Jin, P. J., & Chen, Y. (2020). Porous Pd-PdO Nanotubes for Methanol Electrooxidation. *Advanced Functional Materials*, 30(21), 2000534. <https://doi.org/10.1002/adfm.202000534>
- Xie, J., Feng, N., Wang, R., Guo, Z., Dong, H., Cui, H., Wu, H., Qiu, G., & Liu, X. (2020). A

Reusable Biosorbent Using Ca-Alginate Immobilized *Providencia vermicola* for Pd(II) Recovery from Acidic Solution. *Water, Air, and Soil Pollution*, 231(36).
<https://doi.org/10.1007/s11270-020-4399-z>

Yang, Q., Dou, F., Liang, B., & Shen, Q. (2005). Studies of cross-linking reaction on chitosan fiber with glyoxal. *Carbohydrate Polymers*, 59, 205–210.
<https://doi.org/10.1016/j.carbpol.2004.09.013>

Yi, S. S., Lee, D. H., Sin, E., & Lee, Y. S. (2007). Chitosan-supported palladium(0) catalyst for microwave-prompted Suzuki cross-coupling reaction in water. *Tetrahedron Letters*, 48, 6771–6775. <https://doi.org/10.1016/j.tetlet.2007.07.093>

Appendix

XPS data

Table 4.A1: C1s XPS spectra of Pd@GCC	
XPS peak	Interpretation
284.84	C-C/C-H
286.32	C-O-C, C-OH, C-O, C-NH ₂
287.65	C=O
288.73	O-C-O, O-C=O
Table 4.A2: N1s XPS spectra of Pd@GCC	
XPS peak	Interpretation
399.20	O=C-NH
400.63	C-N
402.46	NH ₂ -Pd
Table 4.A3: O1s XPS spectra of Pd@GCC	
XPS peak	Interpretation
529.64	Surface Oxygen
530.61	Pd-O
531.51	N-C=O

Optimization of Catalyst amount

Reaction with 1.59 mmol Iodobenzene and Phenylboronic acid requires more catalyst for the completion of the reaction with but 3 mg catalyst at 100 °C and gave 99% yield.

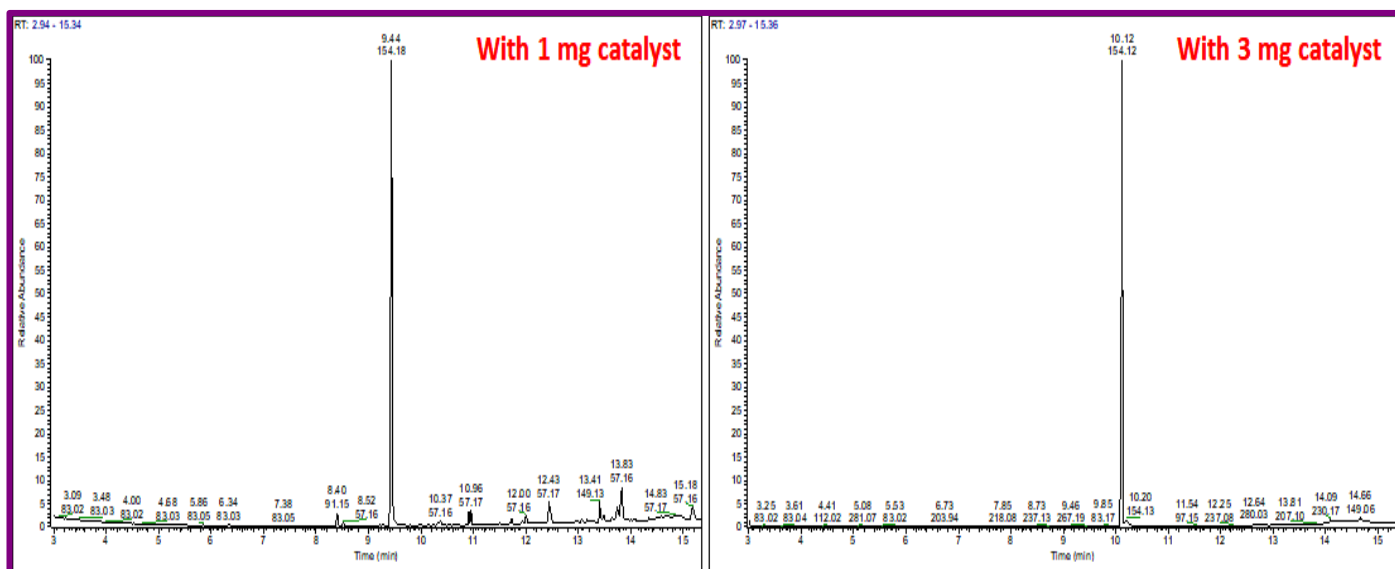


Figure 4.A2: GC-MS spectra of the product for Pd@GCC catalysed reaction between Iodobenzene and phenylboronic acid performed using K_2CO_3 and water as a solvent at 100 °C

Optimization of temperature

It was observed that coupling of 1.59 mmol Iodobenzene and Phenylboronic acid was studied at different temperatures from 100 to 30 °C (i.e, Room temperature) with 3 mg of Catalyst.

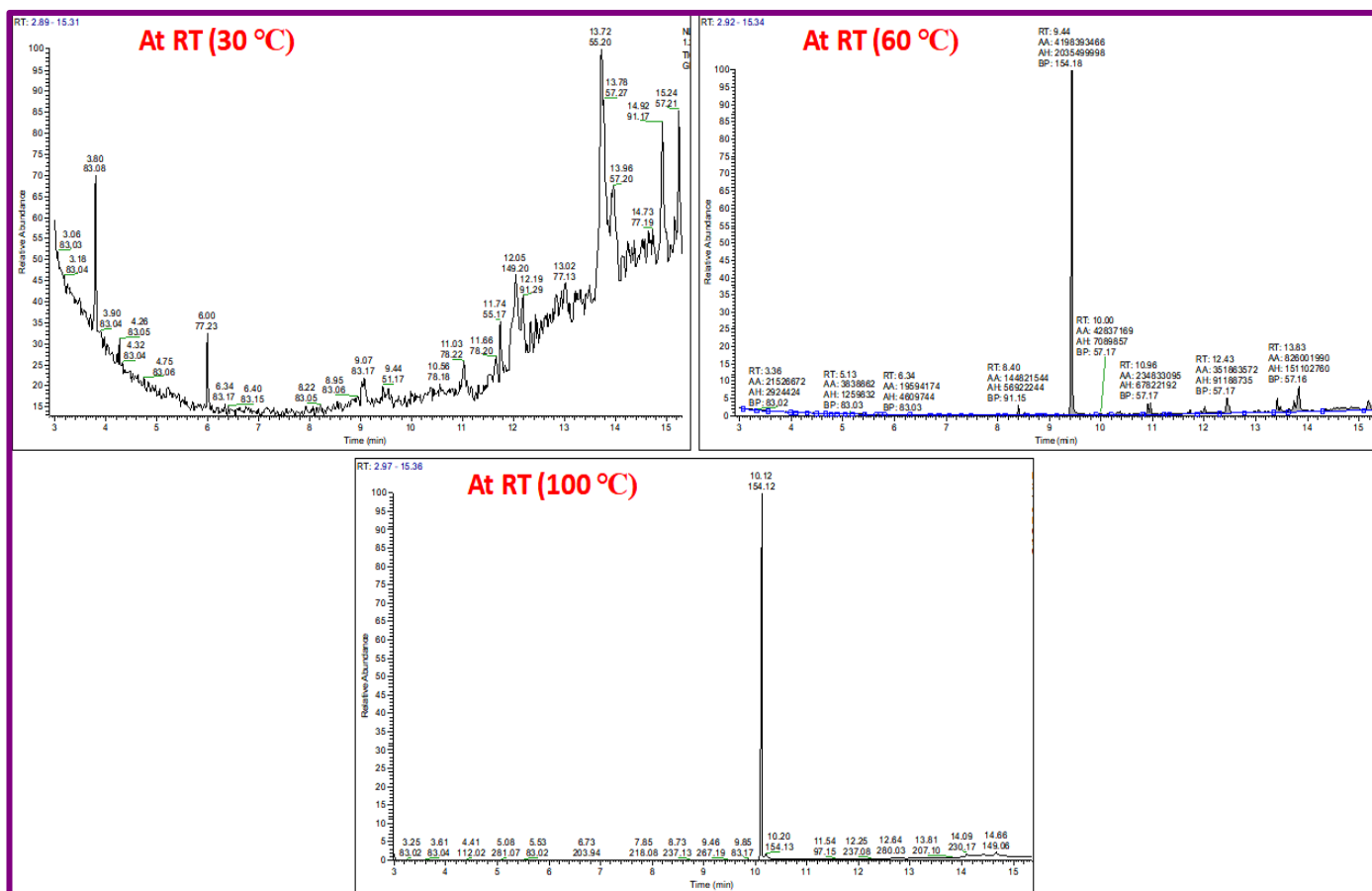


Figure 4.A3: GC-MS spectra of the product for Pd@GCC catalysed reaction between Iodobenzene and phenylboronic acid performed using K_2CO_3 and water as a solvent at 30, 60 and 100 °C

Optimization of Base

Screening of bases such as K_2CO_3 , Na_2CO_3 , NaOH and KOH was performed and it revealed that highest yield could be obtained by the use of 2 equiv. K_2CO_3 as base.

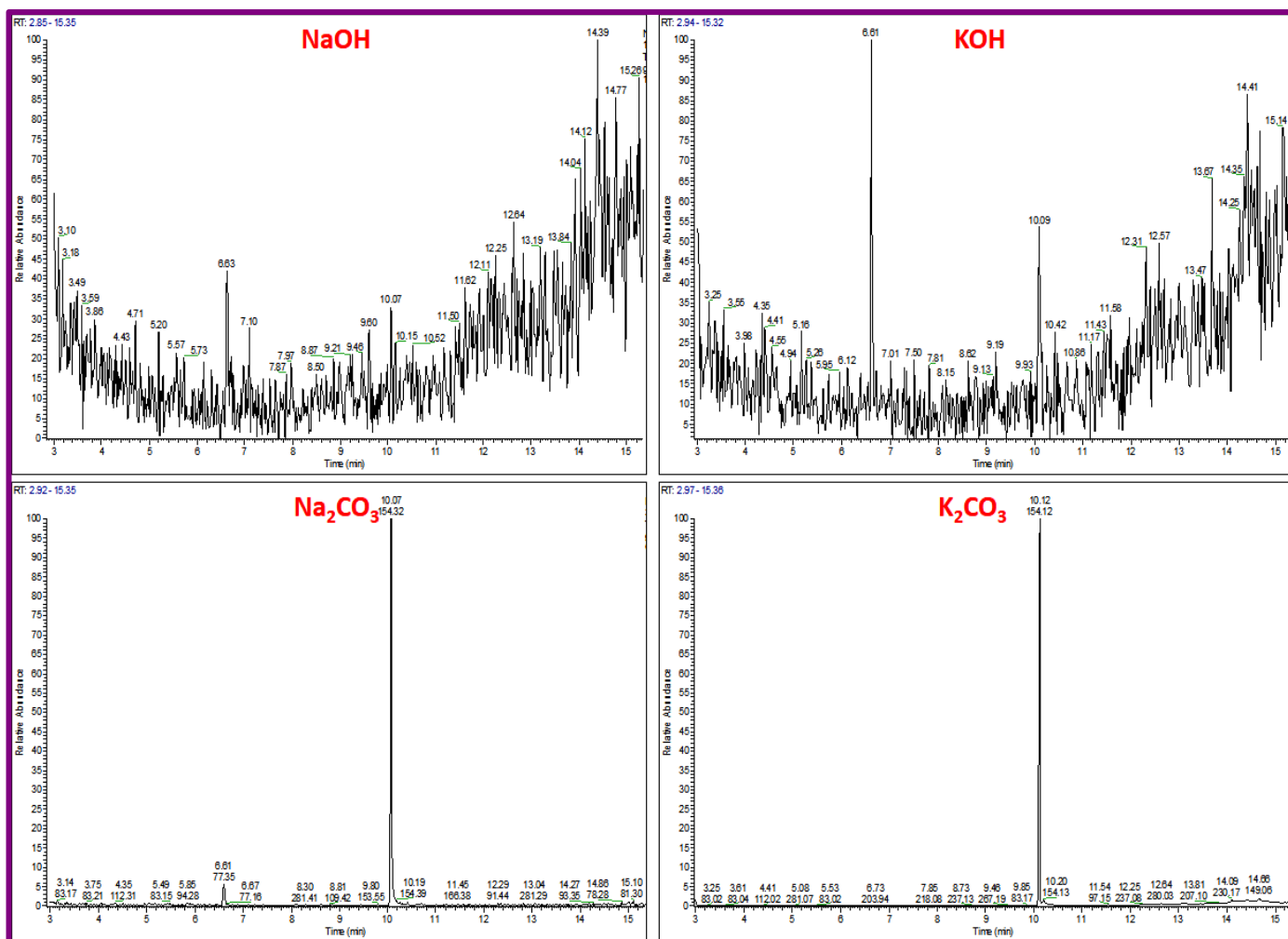


Figure 4.A4: GC-MS spectra of the product for Pd@GCC catalysed reaction between Iodobenzene and phenylboronic acid performed using NaOH, KOH, K_2CO_3 , Na_2CO_3 and water as a solvent at 100 °C

GC-MS spectra of biphenyl derivatives obtained by using Pd@GCC catalyst

Figure 4.A5: GC-MS spectra of crude product synthesized From Aryl halides and Phenylboronic acid at 100 °C using Pd@GCC catalyst

Recyclability

Recycling of catalyst was carried out using Iodobenzene (1.59mmol), Phenyl boronic acid (1.59 mmol), K_2CO_3 (3.18 mmol), Pd@GCC (3 mg) and H_2O (10 ml) at $100^\circ C$ under stirring.

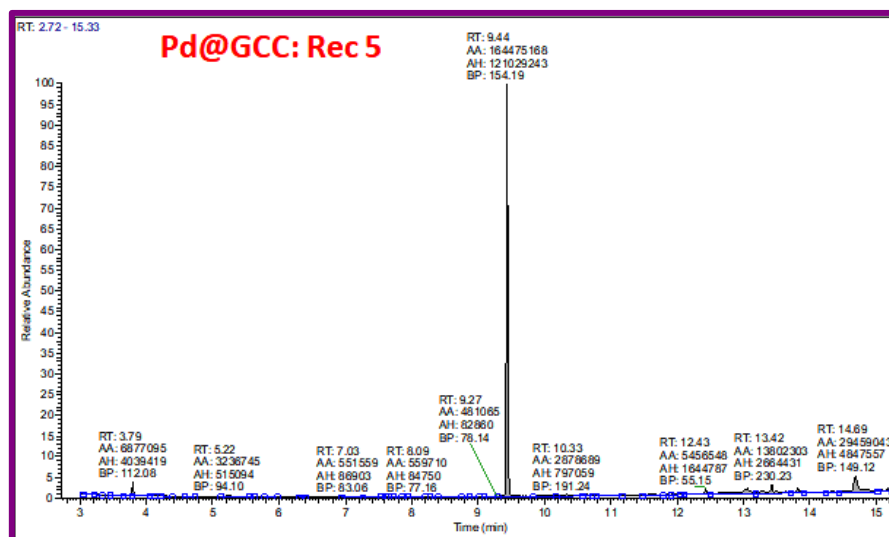


Figure 4.A6: GC-MS spectra of the product for Recycled catalyst (Pd@GCC & Pd@GCC-r) catalysed reaction between Iodobenzene and Phenylboronic acid performed at $100^\circ C$